IOP Publishing | Bureau International des Poids et Mesures Metrologia

Metrologia **52** (2015) 244–250 doi:10.1088/0026-1394/52/2/244

A simple method for high-precision calibration of long-range errors in an angle encoder using an electronic nulling autocollimator

Mark N Kinnane[1], Lawrence T Hudson[1], Albert Henins[1] and Marcus H Mendenhall[1,2]

[1] National Institute of Standards and Technology (NIST), Gaithersburg, MD 20899-8422, USA
[2] School of Engineering, Vanderbilt University, PO Box 351816 Station B, Nashville, TN 37235, USA

E-mail: marcus.mendenhall@nist.gov

Received 6 October 2014, revised 12 January 2015
Accepted for publication 14 January 2015
Published 9 March 2015

Abstract

We describe a simple method for high-precision rotary angle encoder calibration for long-range angular errors. By using a redesigned electronic nulling autocollimator, an optical-polygon artifact is calibrated simultaneously with determining the encoder error function over a rotation of 2π rad. The technique is applied to the NIST vacuum double crystal spectrometer, which depends on precise measurement of diffraction angles to determine absolute x-ray wavelengths. By oversampling, the method returned the encoder error function with an expanded uncertainty ($k = 2$) of 0.004 s of plane angle. Knowledge of the error function permits the instrument to make individual encoder readings with an accuracy of 0.06 s ($k = 2$), which is limited primarily by the least count and noise of the encoder electronics. While the error function lay within the nominal specifications, it differed from the intrinsic factory curve, indicating the need for *in situ* calibration in high-precision applications.

Keywords: angular metrology, angle, autocollimator, encoder, x-ray, xrd, circle closure

(Some figures may appear in colour only in the online journal)

1. Introduction

The practice of metrology-grade x-ray diffraction requires precise and verifiable measurements of angles. Such measurements are typically carried out using a high-precision optical encoder coupled to the rotary stage which sets the angles. For standards work, the ability to verify performance *in situ* is critical to ensure correct installation and to establish traceability. It is widely known that beneath the vendor-stated error bounds on angular accuracy is a stable, slowly varying structure (in the sense that a Fourier series with a modest number of terms is a suitable representation). The long-range angular error function of the encoder is the sum of intrinsic aberrations (the factory calibration curve) and possible additional structure that is introduced upon assembly and is the result of imperfect alignment between the encoder and the rotation stage. The purpose of the present work is to characterize this static *in situ* encoder error function to greatly reduce the uncertainty budget in x-ray diffraction applications. This work does not determine the very short-period errors in the encoder due to interpolation between individual optical marks. As noted below, depending upon the measurement tools employed, it is possible for this method to be sensitive to such short-range errors, or determine if they have been sufficiently compensated by the read-out system; this would appear as increased residuals. Of course short-range errors must be addressed and such is the subject of a forthcoming publication.

The method presented here extends the dual closure method of Estler [1] that was used to calibrate discrete-angle indexing tables. In closure techniques, the fact that a set of

discrete steps around a full circle have all the angles add up exactly to 360 degree creates a closing equation to a set of otherwise incomplete simultaneous equations describing the angle differences of faces of arbitrary polygons. This allows one to collect various sums of angles around full rotations and solve for the individual angles. The primary measurands in this work are the reported angle positions of the face normals of a regular mirrored polygon as registered with an electronic nulling autocollimator. The data analysis is presented in a succinct and mathematically precise form, as a system of linear equations, such that it can be easily solved and broadly applied. This formulation results in very simple error propagation, since only one linear-least-squares solution is used and its variance-covariance matrix directly provides the correct errors. Since the polygon face deviations from their nominal exterior angle and encoder errors are determined together in a single step, the uncertainty analysis is simplified by the lack of need to handle correlated errors in the positions of the sides of a separately-calibrated polygon. The procedure does not demand any particular knowledge or uniformity of the artifact, only that it be stable over the time during which the measurements are made. The result is a highly-accurate angle-dependent error function for a rotary encoder that replaces the vendor-quoted uncertainty bounds and intrinsic factory-calibration.

This calibration method is applied to the goniometer and encoder assembly of the NIST vacuum double crystal spectrometer used to measure absolute x-ray wavelengths [2, 3]. This application seeks an uncertainty in wavelength determination better than 0.3 femtometre, which in turn requires an angle uncertainty of order 0.1 s. Besides a rigorous description of a solution to the problem, we document the tools that were used at NIST to carry out this demonstration. This includes especially the current implementation of the NIST nulling autocollimator, so that the device and the technique can be replicated.

Note on notation: in this paper, we will use the symbol '″' and the spelled-out word 'second' exclusively to refer to seconds of plane angle.

1.1. Brief history

Calibration of goniometers has an extremely long history, driven originally by the need for measuring angles in astronomy to very high accuracy. This problem has being addressed in various forms for more than two centuries and the fundamentals have changed only modestly over this span. The concept of circle closure has been used at least since 1809 [4] by Edward Troughton, who cites work by his brother, John Troughton, from 1775 and alludes to work by Robert Hooke (presumably a century earlier). In Troughton's work, the artifact is a roller which is roughly matched to roll an integral number of times around the circle to be calibrated, but which is never exact and which he then proceeds to show how circle closure can be used to correct it to make a much better full-circle scale. Much more recently, Cook [5] describes calibrating an optical polygon by exactly solving a set of equations for angular differences between its faces.

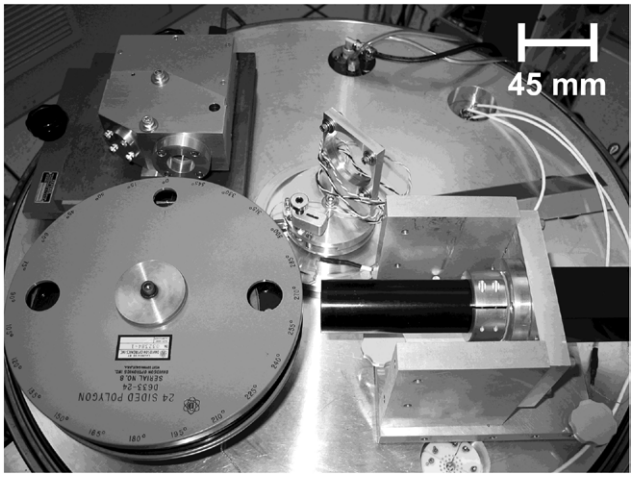

Figure 1. Photograph of the apparatus used for encoder calibration.

Although this technique is formally correct, it is subject to correlated errors and many modern authors [6–8] have recognized the importance of overdetermined systems and least-squares solutions to allow some robustness against all the results being dependent on the point-to-adjacent-point experimental uncertainty of each measurement. In [6], the calibration is carried out in two steps, the first being the calibration of a magnetic scale artifact, which is then transferred to the actual encoder under test. The methods of papers such as [6, 7, 9] take advantage of data from multiple read heads to provide some of the fixed angles useful in a closure, which requires specially-built encoders and electronics, which this work does not require. In [8], a number-theoretic prime-factor algorithm is used to effectively sample a higher harmonic number than would be achieved by the direct measurements described herein. This may have benefits in the case of a system which requires a very high number of Fourier terms, but the Fourier series of error terms converges sufficiently rapidly in the tests we describe that the extra complexity does not appear justified. A noteworthy, general paper about self-consistent calibrations of almost anything (angles, lengths, disc sanders, etc) is [10]. The self-consistent methods described therein for angles are closely related to circle closure.

2. Apparatus

Figure 1 shows a photograph of the main components used for encoder calibration. Figure 2 shows a top–down schematic with some nominal relative angles indicated. The apparatus consists of a Davidson Optronics model D633-24[3] fused-quartz, twenty-four-sided, optical polygon coupled to a Heidenhain RON905 encoder via a shaft passed through a rotary table. An offset measuring autocollimator

[3] Certain commercial equipment, instruments, or materials are identified in this paper in order to specify the experimental procedure adequately. Such identification is not intended to imply recommendation or endorsement by the US government, nor is it intended to imply that the materials or equipment identified are necessarily the best available for the purpose.

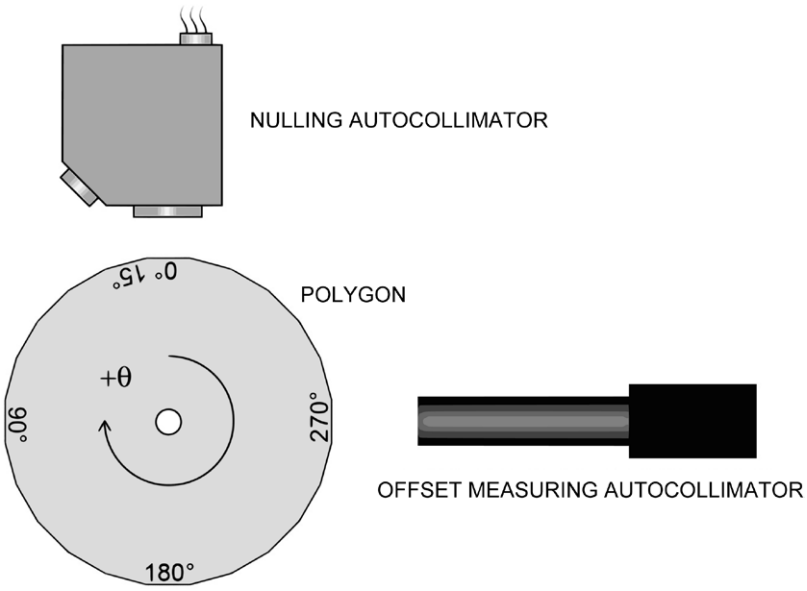

Figure 2. Schematic of the apparatus used for the encoder calibration. The positive direction of rotation is indicated by $+\Theta$. The distance from the nulling autocollimator window to the polygon faces is approximately 30 mm. The distance from the offset measuring autocollimator window to the polygon faces was approximately 20 mm. The twenty-four polygon face angles are nominally separated by 15°.

and a nulling autocollimator are placed on the table top with probe beams incident upon orthogonal polygon faces to measure polygon face orientation. The nulling autocollimator measures the relative encoded angle of each polygon face as the face is rotated past the fixed viewing direction of the nulling autocollimator (figure 4). The offset measuring autocollimator is used to monitor polygon precession out of the plane of rotation by recording the mirrored face elevations.

The spectrometer table is mounted on a twenty tonne concrete slab located beneath the laboratory floor. Air cushions between the slab and the basement floor vibrationally isolate the entire apparatus from the laboratory floor and surroundings. The laboratory is located over 12 m below ground level in an advanced-measurement laboratory designed to also limit excursions in room temperature. Laboratory temperature control is required to minimize mechanical shifts of spectrometer components. Extended monitoring indicated a standard deviation in laboratory temperature of 0.05 °C over thirty days.

2.1. Encoder/stator assembly

A 28.4 mm diameter shaft passes through the axes of rotation of a Huber stator, driven by a NIM dual microstepper and a Heidenhain RON905 encoder. Both devices are coupled to the shaft so that the stator provides simultaneous polygon and encoder optical disc rotation. Stepping-motor pulses are generated by a Kinetic Systems 3360 pulse generator controlled by LabVIEW software. The microstepper generates 10 000 pulses per degree of rotation giving a step resolution of 0.36″ per pulse. Relative encoder angle is reported by a Heidenhain AWE1024 angle interpolator, which produces 102 400 counts per degree of rotation. The factory guaranteed position accuracy of the encoder-interpolator system is ± 0.2″ and an error function, measured under ideal conditions, is provided with the device which supports this guarantee.

2.2. Polygon characteristics

The twenty-four sided polygon diameter (face to opposing face) is 206 mm and the height of each face is 25 mm. Imperfections in manufacture contribute deviations of up to ± 6″ from the nominal 15° angle between adjacent faces; these deviations are determined experimentally as described later. Face tilts out of the plane of rotation are within ± 4″ of the rotation axis. Care must be taken to ensure polygon imperfections or errors in the polygon's mounting axis relative to its rotation axis contribute negligibly to nulling autocollimator cross talk errors (defined and discussed in section 2.4.2).

2.3. Offset measuring autocollimator

An offset measuring autocollimator is used to measure the angular difference between the normal of a flat mirrored surface and its line of sight. The autocollimator is a Micro-Radian 240L dual axis laser system, customized to accommodate an angular range of ± 500″ and is mounted on a three-point kinematic table. The offset measuring autocollimator is primarily used to manage crosstalk errors.

2.4. Nulling autocollimator

The nulling autocollimator was designed and constructed by NIST. An earlier version which operates on the same

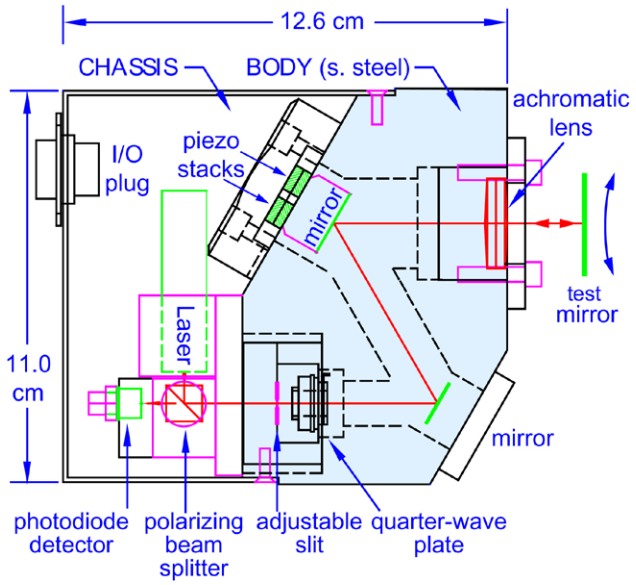

Figure 3. Internal schematic of the nulling autocollimator.

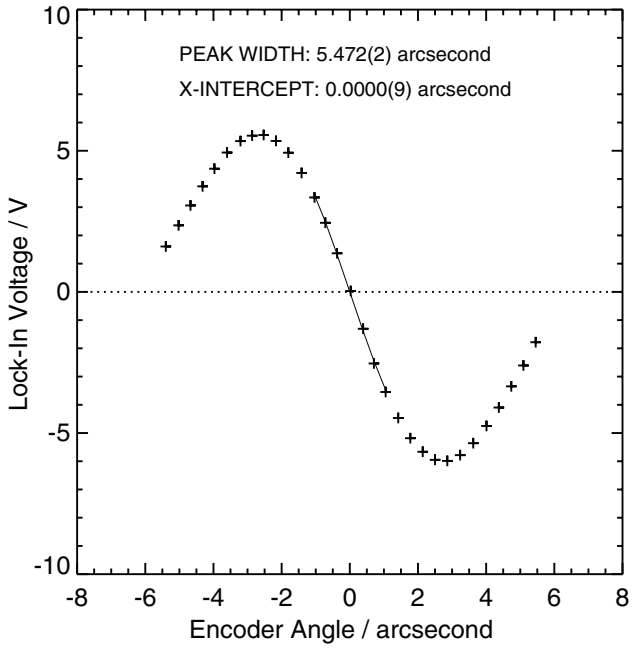

Figure 4. Characteristic curve produced by rotating an external reflecting surface past the NIST nulling autocollimator. A 'nulled' fiducial point is defined by the encoder angle at which the derivative of the central lobe crosses 0 V. The abscissa is usually a relative encoder angle, but is shown offset to 0.

principles, but lacks several recent optimizations, is described in detail elsewhere [11]. The nulling autocollimator presently employs a laser light source instead of a pin-light lamp that was used in the earlier version. Use of a solid-state light source provides much greater illumination of the test mirror with little susceptibility to thermal fluctuations. Alignment of the earlier version was somewhat difficult as the outgoing and return beams could not overlap at the adjustable slit and so were offset vertically. By introducing a polarizing beam splitter the outgoing and return beams can overlap at the adjustable slit which simplifies alignment and allows simple quantification of crosstalk errors described later. Figure 3 shows an internal construction schematic of the upgraded nulling autocollimator.

A laser beam of 660 nm wavelength is reflected and vertically polarized by a polarizing beam splitter before collimation by a vertical slit. The beam is right-circularly polarized by a quarter wave plate, reflected from a stationary mirror onto a piezo-controlled rocking mirror and then passes through an achromatic lens. The beam path length from the slit to the achromatic lens is equal to the lens focal length. This configuration generates a parallel output beam incident upon an external reflecting surface (test mirror of figure 3). The vertical slit produces a single slit diffraction pattern that propagates from the slit to the lens. The vertical-slit collimator width (3 μm) is chosen so that, after reflection, the central lobe of the resulting single slit diffraction pattern is the same width as the achromatic lens when the beam reaches the lens plane. The internal rocking mirror is mounted on a piezoelectric stack which moves the mirror about a central axis at a frequency determined by a lock-in amplifier reference signal described later.

The return beam from the test mirror has passed through the quarter-wave plate twice, producing a 90 degree polarization rotation. This allows the return beam to be separated from the outgoing beam by the polarizing beam splitter and detected by the photodiode.

2.4.1. Autocollimator electronics. The autocollimator system consists of a lock-in amplifier driving the autocollimator via an audio power amplifier, with the resultant detected signal from the lock-in being acquired by the control computer. A 6.5 V_{p-p} reference signal from the lock-in amplifier drives the rocking mirror oscillation. The photodiode output voltage provides the input signal to the lock-in amplifier. If the test mirror deflects the probe beam away from its original path then the center of beam oscillation, at the plane of the collimating slit, will not lie on the slit itself. This causes a phase shift between the input signal and the reference signal. The lock-in amplifier first harmonic quadrature (90°) output signal is proportional to the sine of the phase shift between the reference signal and the input signal. Therefore the output signal voltage is null only when the probe beam is nominally perpendicular to the mirror, providing a very precise fiducial. If the amplitude of motion of the diffraction pattern across the slit is small compared to the diffraction pattern central lobe width, the in-phase (0_o) output signal can equivalently be treated as proportional to the intensity pattern derivative. This is the mode of operation used for the rest of this paper.

2.4.2. Nulling autocollimator characterization. Figure 4 shows a typical lock-in amplifier output signal as a single polygon face rotates through the nulling autocollimator probe beam. Encoder angle is recorded by the Heidenhain RON905 encoder as the polygon is rotated through approximately 12″. In effect, the curve of figure 4 is the derivative of the central lobe of the nulling autocollimator single slit diffraction intensity profile. The angular separation between the minimum and maximum voltages of figure 4 represents the full width at half maximum of the central lobe. In this case the peak width is approximately 5.5″.

The encoded angle at which the test mirror normal is parallel to the autocollimator probe beam, the null angle (indicated by the 0 V crossing point (x-intercept) of figure 4), is determined by a linear fit to six central curve points. The six central points are chosen for fitting as points beyond this range deviate from linear behavior. The fit of a single curve (one pass of the mirror through the beam) results in a fitted null angle uncertainty of approximately ± 0.0009″(k = 1), ignoring the systematic contribution due to the least count of the encoder. The least count of the encoder does not contribute to any systematic bias in the system, since the oversampling of the data at slightly randomized angles (due to the polygon rotation) dithers over such bias.

Crosstalk is the aliased or apparent shift in the null angle due to a non-zero elevation angle of the reflecting mirror coupled with imperfections in the collimating slit of the nulling autocollimator. The intrinsic nulling autocollimator crosstalk error is quantified by measuring changes in a single fitted null angle as the elevation angle is varied. Monitoring of the deviation of each polygon face from vertical using the offset measuring autocollimator ensured crosstalk errors of measured polygon dihedral angles were suppressed to less approximately 0.01″.

3. Calibration of angles

3.1. Procedure

Encoder calibration is undertaken using a stable, uncalibrated angle artifact; in this case, a mirrored polygon. In the method described below, we use circle closure and the uncalibrated encoder to simultaneously calibrate the angle artifact and the encoder.

For nearly regular polygons with n sides, the angle θ_m of the face m relative to a reference face is (in radians)

$$\theta_m = \frac{2\pi m}{n} + \epsilon_m, \tag{1}$$

where ϵ_m represents the small deviation of the face angle from the nominal value. For the reference face, $\epsilon_1 \equiv 0$.

The procedure begins with unclamping the polygon from the encoded axis, rotating it and re-clamping it, with a rotation angle ϕ_k relative to the encoder stage. The rotation angles ϕ are chosen such that a wide range of angles are sampled around an entire 360 degrees. For each of the K values of ϕ_k, the encoded axis is then rotated itself through 360 degrees such that each face angle of the polygon, indexed by m, is measured using the nulling autocollimator (as in figure 4). The fitted null positions, as measured by the encoder, resulting from this repeated phasing of the artifact with respect to the encoder, are the primary measurands: $\psi_{m,\,k}$. If the error function is to be modeled by a Fourier series with p harmonics, a minimum set of ϕ_k would divide the circle into at least $2p$ parts. Since we will carry out the fit using least squares and not a discrete Fourier transform, there is no requirement that the samples be perfectly uniformly spaced.

Once the apparent angles $\psi_{m,\,k}$ data have been determined, they can be related to the real rotation angles, given by $\theta_m + \phi_k$, by the addition of the encoder error function:

$$\psi_{m,k} = \frac{2\pi m}{n} + \epsilon_{m \bmod n} + \phi_k + \sum_{h=1}^{p} A_h \cos h\psi_{m,k} + B_h \sin h\psi_{m,k}, \tag{2}$$

with the A_h, B_h, ϵ_m and ϕ_k all as unknowns. Note that this is a linear system of equations, making it easy to solve with only the additional constraint that $\epsilon_1 \equiv 0$ and making error analysis straightforward. Also note that, for a given ϕ_k, it may be useful to make multiple full turns of the stage to improve the statistics; if such is the case, the index m may run larger than the n sides of the polygon. This is the reason (2) uses $\epsilon_{m \bmod n}$ (a trivial statement of circle closure). There is no specific requirement that the datasets associated with each ϕ_k be the same length or that they consist of entirely complete turns, as long as the resulting system of equations is sufficiently overdetermined.

Also, note that the face angle errors ϵ_m from this method are only to be interpreted within the requirement of self-consistency in the particular calibration setup. The polygon may well have face flatnesses which could cause larger angular errors than this if it is mounted and measured differently. For example, realigning the autocollimator such that it is reflecting from a different horizontal or vertical position on the polygon may result in different face angle errors. As long as this is not done during a measurement of the encoder errors, it does not affect the encoder error computation.

The system of equations represented by (2) can be solved by creating a matrix of the form (where the top row just shows how the columns are indexed):

$$M = \begin{Bmatrix} 1 & 2 & 3 & 4 & \dots & 2p & 1 & 2 & \dots & n & 1 & 2 & \dots & K \\ \cos\psi_{1,1} & \sin\psi_{1,1} & \cos 2\psi_{1,1} & \sin 2\psi_{1,1} & \dots & \sin p\psi_{1,1} & 1 & 0 & \dots & 0 & 1 & 0 & \dots & 0 \\ \cos\psi_{2,1} & \sin\psi_{2,1} & \cos 2\psi_{2,1} & \sin 2\psi_{2,1} & \dots & \sin p\psi_{2,1} & 0 & 1 & \dots & 0 & 1 & 0 & \dots & 0 \\ \vdots & & & & & & & & & & & & & \\ \cos\psi_{1,2} & \sin\psi_{1,2} & \cos 2\psi_{1,2} & \sin 2\psi_{1,2} & \dots & \sin p\psi_{1,2} & 1 & 0 & \dots & 0 & 0 & 1 & 0 & \dots \\ \vdots & & & & & & & & & & & & & \\ \cos\psi_{n,K} & \dots & & & & \sin p\psi_{n,K} & 0 & 0 & \dots & 1 & 0 & 0 & \dots & 1 \\ 0 & 0 & 0 & 0 & 0 & 0 & 100000 & 0 & 0 & 0 & 0 & 0 & 0 & 0 \end{Bmatrix}. \tag{3}$$

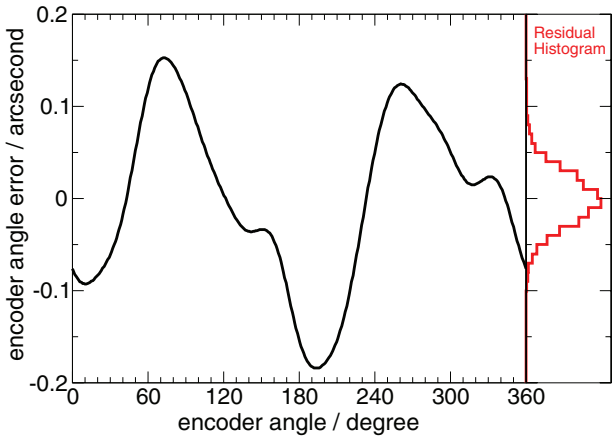

Figure 5. Plot of computed encoder angular error correction (the ∑ term from (2)) and histogram of residuals from fit. Note that the uncertainty in the fit function is not much wider than the line plotted ($k = 2$ expanded statistical uncertainty = 0.004″). The function is within the stated factory specifications of ± 0.2″.

Then, we define the solution vector, written as a row for typographical convenience, but which will be used as a column,

$$\alpha = \left\{A_1 \;\; B_1 \;\; A_2 \;\; B_2 \;\; \ldots \;\; B_p \;\; \epsilon_1 \;\; \epsilon_2 \;\; \ldots \;\; \epsilon_n \;\; \phi_1 \;\; \phi_2 \;\; \ldots \;\; \phi_K\right\}, \tag{4}$$

and the data vector (which is also a column vector)

$$Y = \left\{\psi_{1,1} - \frac{2\pi}{n} \;\; \psi_{2,1} - \frac{4\pi}{n} \;\; \ldots \;\; \psi_{n,K} - \frac{2\pi n}{n} \;\; 0\right\}. \tag{5}$$

The last row in each of M and Y pins ϵ_1 to 0, making the system solvable and assigning a sufficiently high weight to that equation that the resulting solution is easier to interpret. One could also do this by explicitly eliminating it from the equations, but adding a row to the matrix is easy and leaves the underlying equations very symmetric and easy to program. Also, note that if $2p = n$, i.e. one is solving for the full Nyquist limit of frequencies, the $\sin p\psi$ column must be dropped since it is undefined.

The solution is found by solving

$$M\,\alpha = Y, \tag{6}$$

using the linear systems solver available in the software package in which the analysis is implemented.

3.2. Data analysis

For the present demonstration, the calibration data consisted of registering the autocollimator's null (measurand ψ) for each face of the polygon (m) at values of ϕ_k spaced at approximate 15 degree intervals around the circle and some extra positions at approximately 1.5 degree values between 0 and 15 degrees. A total of 38 ϕ_k and 4588 $\psi_{m,\,k}$ angles were included in the fit. The uncertainty of the each measurement was assumed to be identical and was adjusted to get a reduced χ^2 of 1, resulting in $\sigma = 0.03''$. The residuals have no discernible structure and have a nearly ideal Gaussian distribution (see red curve on right of figure 5). This provides support for an assumption that all errors can be treated as type A contributions to the uncertainty [12] and provides evidence that a sufficient number of harmonics has been included in the series to represent the data. It is important to note that self-consistent measurements of dimensionless quantities can be made with no formal type B contributions to the uncertainty, since the requirement of consistency effectively cancels them out [10]. For comparison, the least count on the encoder was 1°/102 400 ≈ 0.035″. With a 24-sided polygon, the Nyquist limit for the Fourier series would include up to the 12th harmonic; however, the 12th harmonic is poorly determined, so we present an 11 harmonic fit.

Note that, since the polygon we use has face angles very close to an integral multiple of the 0.01° spacing of the optical features on our encoder, the short period, so-called 'compensation' function, does not appear in this, since on any given setting of the polygon mounting angle, we sample the compensation function at the same phase for every face. If we were to have a polygon with face angles which were not close to multiples of the encoder feature spacing, it would show up as a lack of self-consistency and increase the residuals of the fit. However, as long as a sufficient set of random polygon mounting angles is chosen, it still should not bias the determination of the long-range encoder error function.

The fitted parameters (except for the ϕ_k) are shown in tables 1 and 2. The fit function and histogram of residuals are shown in figure 5.

Some features of these results are noteworthy:

Table 1. Fourier coefficients A_h and B_h for correction (see (2)). Uncertainties are $k = 1$ statistical errors.

Frequency, h (turn^{-1})	Cos Ampl. $A_h(''$)	Sin Ampl. $B_h(''$)
1	−0.0433(6)	−0.0059(6)
2	0.1119(6)	0.0124(6)
3	0.0054(6)	−0.0069(6)
4	−0.0082(6)	0.0468(6)
5	−0.0015(6)	−0.0007(6)
6	0.0008(6)	0.0031(6)
7	0.0006(6)	−0.0010(6)
8	0.0083(6)	0.0006(6)
9	0.0008(6)	−0.0008(6)
10	0.0023(6)	−0.0005(6)
11	−0.0008(6)	0.0004(6)

Table 2. Self-consistent polygon face angle errors ϵ_m (see (1)). Uncertainties are $k = 1$ statistical errors.

Face m	ϵ_m (″)	Face m	ϵ_m (″)
1	0.000(0)	2	1.320(3)
3	1.290(3)	4	1.177(3)
5	1.306(3)	6	1.198(3)
7	3.067(3)	8	1.750(3)
9	−1.962(3)	10	1.419(3)
11	3.654(3)	12	1.350(3)
13	−0.991(3)	14	0.658(3)
15	0.379(3)	16	2.220(3)
17	−1.626(3)	18	0.788(3)
19	0.576(3)	20	2.365(3)
21	−3.005(3)	22	−1.257(3)
23	2.246(3)	24	−0.860(3)

Note: Face 1 is defined to have zero angle. Note that these are only to be interpreted as valid for a given alignment of the polygon and autocollimator. The polygon itself may produce different deviations due to face flatness, etc if it is aligned differently.

- Our encoder was mounted within tolerance for each vendor-specified degree of freedom and the resulting error function was found to fall within the nominal error bounds for this encoder, ± 0.2″ (figure 5).
- The $k = 2$ uncertainty associated with the error function in figure 5 is only 0.004″, reflecting the high degree of oversampling in our data acquisition. Of more practical import is the histogram of the residuals, plotted to the right of the error function. This histogram is found to be a Gaussian distribution with $\sigma = 0.03''$, which is nearly equal to the least count of the encoder. In our apparatus, then, the least count is the accuracy limit for a single encoder reading. In most applications, absolute angle determination involves the difference of two encoder readings, which would yield a $k = 2$ expanded uncertainty of 0.08″.
- The encoder was delivered with an intrinsic calibration curve exhibiting mainly 4θ character (and similar in amplitude to the 4θ term we find). The measured curve, however, is dominated by a 2θ term in our result. This demonstrates the need for *in situ* calibration in high precision applications that require encoder performance exceeding the nominal uncertainty specified in the product manual.
- The amplitude of the harmonics decreases rapidly with harmonic number, although not monotonically, towards the limit of significance. Even harmonics are stronger than odd ones.
- Because of limitations intrinsic in Nyquist's theorem for uniformly sampled data, the calibration we present as an example is not capable of determining structure corresponding to harmonics larger than $h = 12$. Sampling more finely or non-uniformly [8, 9 e.g.] could permit higher spatial frequencies to be measured, but the power spectrum in our case is approaching zero rapidly, so there is no obvious evidence of need for this.
- The polyhedron face angle errors in table 2 are completely correlated, so that although they appear to have specific uncertainties only with respect to the reference face, that structure is an artifact. The 0.003″ uncertainty cited is the correct value for the deviation from the nominal face angle. The rotational symmetry of the system results in all of the uncertainties being the same.
- This technique only depends on the stability of the polygon alignment to the autocollimator and not strongly on its absolute face quality. As long as it produces repeatable angle nulls when the autocollimator measures the same face at the same point, this method will return the long-range encoder error function with the precision stated. In this sense, the actual values of the polygon angles are not of primary interest. Failure of this assumption will be manifest in the residuals, since it will not be possible to obtain self-consistent results. This is one advantage of a highly oversampled measurement.

4. Conclusions

A simple procedure is presented for calibrating a very precise angular scale of an angular encoder coupled to a rotation stage and simultaneously calibrating a polygonal reference artifact. The ability to carry out this measurement was assisted by the newly redesigned NIST nulling autocollimator. The method relies on articulating the problem as a straightforward set of linear equations that is soluble by simple matrix arithmetic.

The procedure presented in this paper is recommended for encoded rotary motion applications requiring high accuracy. Although encoders are sometimes shipped with well-measured intrinsic error functions, these can be perturbed by stresses and alignment issues created when the encoder is mounted, even within specified tolerances. In such cases, it is necessary to have an *in situ* measurement of the error function of the coupled encoder and rotation stage.

References

[1] Estler W T 1998 *J. Res. NIST* **103** 141–51
[2] Deslattes R D and Simson B G 1966 *Rev. Sci. Instrum.* **37** 753–4
[3] Deslattes R D 1967 *Rev. Sci. Instrum.* **38** 616–20
[4] Troughton E 1809 *Phil. Trans. R. Soc.* **99** 105–45 (www.jstor.org/stable/107252)
[5] Cook A H 1954 *Br. J. Appl. Phys.* **5** 367
[6] Watanabe T, Fujimoto H and Masuda T 2005 *J. Phys.: Conf. Ser.* **13** 240
[7] Geckeler R D, Fricke A and Elster C 2006 *Meas. Sci. Technol.* **17** 2811
[8] Probst R 2008 *Meas. Sci. Technol.* **19** 015101
[9] Geckeler R D, Link A, Krause M and Elster C 2014 *Meas. Sci. Technol.* **25** 055003
[10] Evans C J, Hocken R J and Estler W T 1996 *CIRP Ann.: Manuf. Technol.* **45** 617–34
[11] Luther G G, Deslattes R D and Towler W R 1984 *Rev. Sci. Instrum.* **55** 747–50
[12] 2008 Uncertainty of measurement–part 3: Guide to the expression of uncertainty in measurement *Technical Report* (Joint Committee for Guides in Metrology) (www.iso.org/sites/JCGM/GUM-introduction.htm)